Progress In Electromagnetics Research Letters, Vol. 98, 33–40, 2021

A Low-Loss Dual-Band Negative Group Delay Circuit with Flexible Design

Yuwei Meng, Zhongbao Wang*, Yu Bai, Shaojun Fang, and Hongmei Liu

Abstract—A low-loss dual-band negative group delay circuit (NGDC) with a flexible design is proposed. The proposed NGDC consists of a transmission line coupled asymmetrically with two step-impedance open-loop resonators. The negative group delay (NGD) times and center frequencies of the lower and upper bands can be tuned independently. To verify the design concept, two dual-band NGDC prototypes I and II are fabricated and measured. The measured NGD times of prototype I are −4.9 ns and −4.8 ns at the center frequencies of 1.949 GHz and 2.054 GHz, respectively. The insertion loss is lower than 2.7 dB and the return loss larger than 11.2 dB in both NGD bands. For prototype II, the NGD times at 1.949 GHz and 2.086 GHz are −4.7 ns and −3.3 ns, respectively. The measured insertion loss is better than 2.4 dB with the return loss larger than 11.9 dB.

1. INTRODUCTION

The distortion of group delay (GD) is one of the challenging issues in a circuit or system, which may distort the signal by introducing inter-symbol interference. Therefore, the GD equalization technique based on the negative group delay circuit (NGDC) arises at the historic moment [1–3]. The traditional NGDCs are usually realized by RLC resonators [4] or transmission line resonators loaded with resistors [5, 6]. Recently, some novel structures have been implemented, such as miniaturization [7], flatness of GD [8], and reconfigurable [9]. However, these NGDCs always suffer from high signal attenuation. So the research on low-loss NGDC has attracted more and more attention [10–13]. Based on lossy transmission lines, signal attenuation can be reduced.

With the rapid development of various wireless systems for multiple-access and multi-functional applications, multiband microwave components that can simultaneously support different communication standards are essential. To satisfy the GD compensation for multiband devices, it is important to increase the number of operation bands of NGDCs. Over the last decade, several dual-band NGDCs have been designed [14–20]. In [14], a dual-band NGDC based on right/left-handed $\lambda/4$ shorted stubs is proposed. However, this circuit works as a reflection-type that necessarily demands a broadband hybrid coupler to realize port-matching. In [15], a two-stage FET-based active circuit is used to produce dual-band negative group delay (NGD). However, the analysis and design of the active circuit are complicated. Therefore, distributed-parameter NGDCs are proposed. In [16, 17], the frequency ratio of the lower and upper bands is controlled by the characteristic impedance of the transmission lines. However, these two NGD center frequencies f_1 and f_2 depend on the center frequency $f_0 = (f_1 + f_2)/2$. To achieve independent controllability, the defected structures are adopted in [18]. The center frequencies of the lower and upper bands can be individually adjusted by a defected microstrip structure and a defected ground structure, while the NGD time can be tuned by changing the loaded resistances. Another dual-band NGDC consists of a couple of open-circuited stubs, whose frequencies of the lower and upper bands are controlled by the length of stubs [19]. However, port matching cannot be

Received 17 April 2021, Accepted 26 May 2021, Scheduled 29 May 2021
* Corresponding author: Zhongbao Wang (wangzb@dlmu.edu.cn).
The authors are with the School of Information Science and Technology, Dalian Maritime University, Dalian, Liaoning 116026, China.

achieved. In [16–19], the insertion loss (IL) is large. To reduce signal attenuation, a dual-band NGDC with three lossy transmission lines and two identical coupled lines is proposed in [20]. However, its two NGD bands cannot be designed separately.

In this paper, a low-loss dual-band NGDC with a flexible design of both NGD bands is proposed. The proposed NGDC is composed of a couple of step-impedance open-loop resonators and a transmission line connecting input/output ports. By asymmetrically coupling the resonators with the transmission line, the dual-band NGD characteristic is realized. The center frequencies of the lower and upper NGD bands (f_1 and f_2) can be tuned independently by the characteristic impedance of the step-impedance resonators without depending on the center frequency f_0. Meanwhile, by tuning the coupling gaps, the individual adjustment of NGD times for both bands can be achieved. The analysis and results of the proposed low-loss dual-band NGDC are given and discussed.

2. DESIGN OF LOW-LOSS DUAL-BAND NGDC

The configuration of the proposed low-loss dual-band NGDC is illustrated in Fig. 1. It consists of two step-impedance open-loop resonators and a transmission line connecting input and output ports. Due to the asymmetrically coupling between the transmission line and the open-loop resonators, the individually-adjusted dual-band NGD characteristic can be realized. The NGD characteristic of the proposed dual-band NGDC is generated by the step-impedance open-loop resonators. Therefore, the NGD time is mainly determined by the width of coupled transmission lines and coupling gaps. The center frequencies of two NGD bands (f_1 and f_2) can be adjusted by the characteristic impedance of the step-impedance resonators without relying on the center frequency f_0.

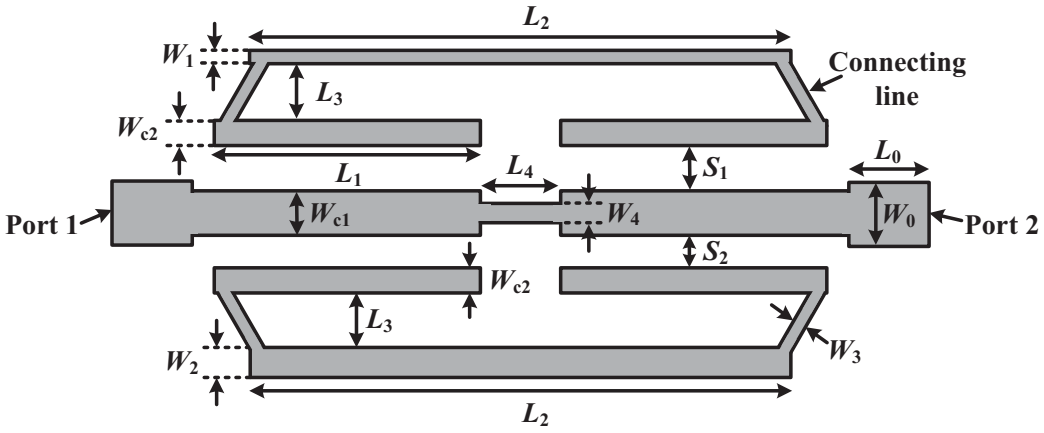

Figure 1. Configuration of the proposed low-loss dual-band NGDC.

Figures 2 and 3 show the effects of the coupling section on the performances of the proposed dual-band NGDC. As shown in Fig. 2, when W_{c1} is increased from 0.8 to 2.8 mm, the NGD absolute values and IL at the center frequencies of both NGD bands are increased with a slight change of $|S_{11}|$ at f_1 and f_2. When W_{c2} is increased from 3.4 to 4.4 mm, both NGD center frequencies are decreased; meanwhile, the NGD absolute values and IL are decreased. As shown in Fig. 3, the gaps of the coupling section S_1 and S_2 have independent effects on the upper and lower bands, and the NGD absolute values and IL at f_1 (f_2) are inversely proportional to S_2 (S_1). Therefore, by tuning S_1 and S_2, the independent adjustment of NGD time for both bands can be achieved.

Fig. 4 gives the effects of W_1 and W_2 (i.e., the characteristic impedance of the step-impedance resonator) on the performances of the proposed dual-band NGDC. When W_1 is decreased from 3.3 to 2.3 mm, the center frequency of the upper NGD band is increased, and that of the lower NGD band is slightly changed. Contrary to W_1, the center frequency of the lower NGD band is increased by decreasing W_2 from 4.8 to 3.8 mm. Thus, W_1 and W_2 can be used to adjust the center frequencies of the upper and lower bands, respectively. Fig. 5 shows the effects of L_1 and L_2. When L_1 or L_2 is decreased,

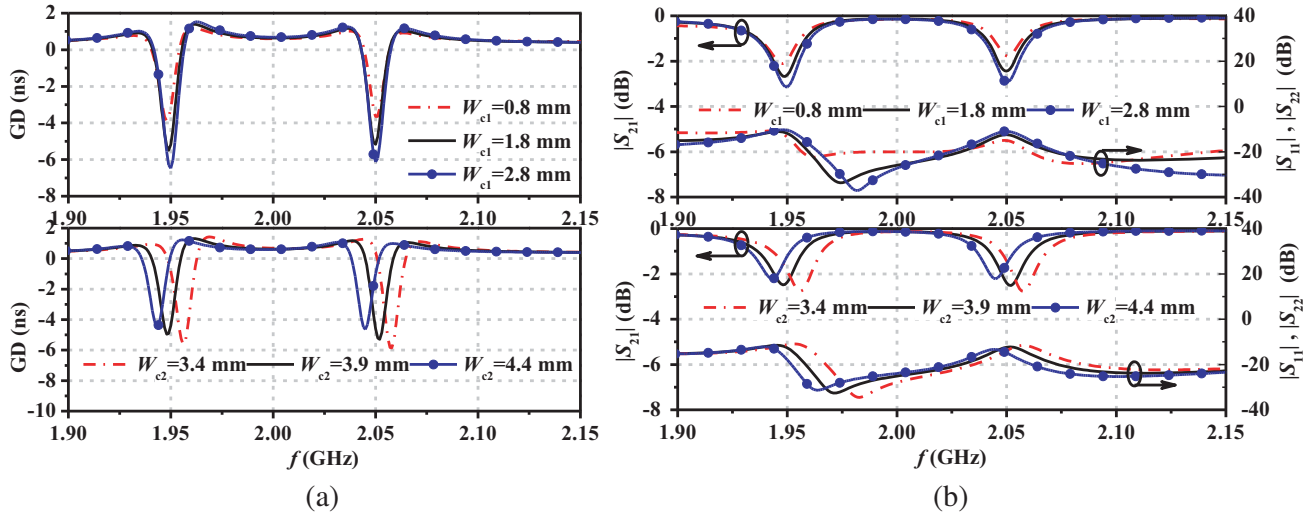

Figure 2. Effect of W_{c1} and W_{c2} on the performances of the proposed dual-band NGDC. (a) GD. (b) S-parameters.

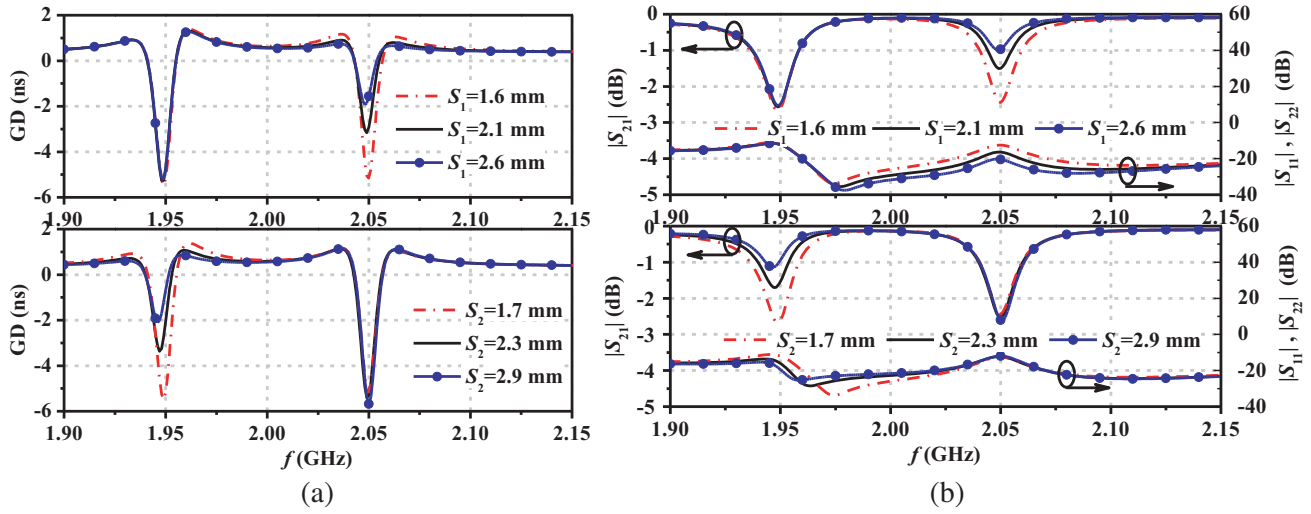

Figure 3. Effect of S_1 and S_2 on the performances of the proposed dual-band NGDC. (a) GD. (b) S-parameters.

both NGD center frequencies are simultaneously increased.

According to the foregoing analysis, the following procedures are suggested to design the proposed low-loss dual-band NGDC.

1) Determine the center frequencies of the lower and upper bands (f_1 and f_2) and the NGD times at f_1 and f_2 according to the design requirements. Obtain the values of relative permittivity and thickness of the substrate.

2) Select proper widths W_{c1}, W_{c2}, W_1, and W_2 referring to Figs. 2 and 4. And calculate the lengths L_1 and L_2 to be about $\lambda/4$ and $\lambda/2$ at $f_0 = (f_1 + f_2)/2$, respectively.

3) Choose proper coupling gaps S_1 and S_2 referring to Fig. 3.

4) Select a proper length L_3 for the connecting lines to ensure that there is no coupling between the microstrip lines with the widths of W_{c2} and W_1 (W_2). And select a proper length L_4 to reduce the coupling between the left and right microstrip lines with the width of W_{c2}.

5) Change L_1, L_2, and W_{c2} in a full-wave electromagnetic simulator to eliminate frequency shift

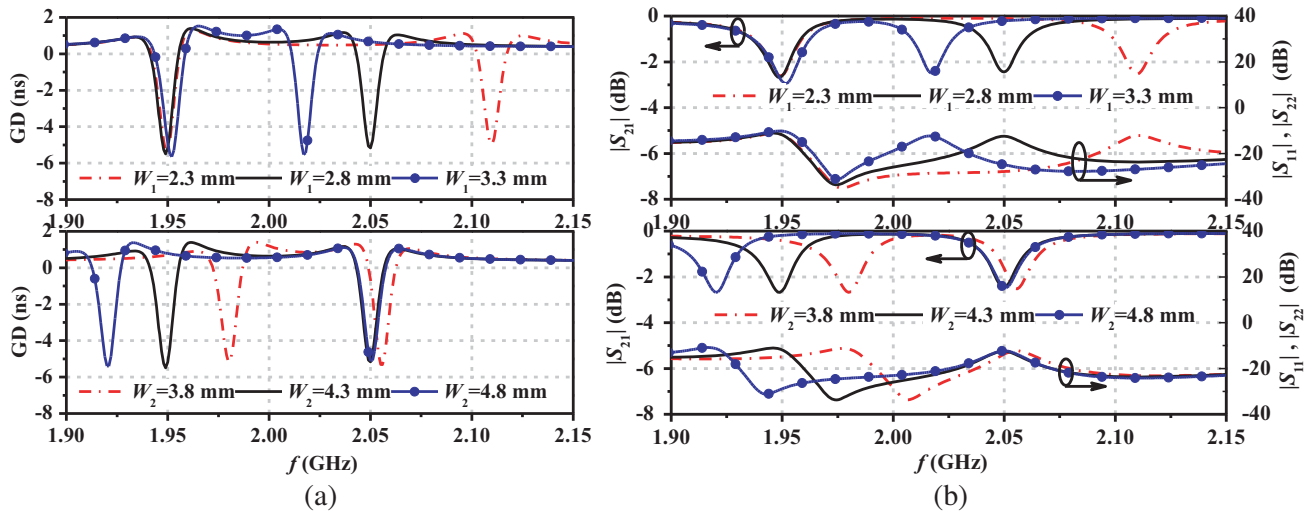

Figure 4. Effect of W_1 and W_2 on the performances of the proposed dual-band NGDC. (a) GD. (b) S-parameters.

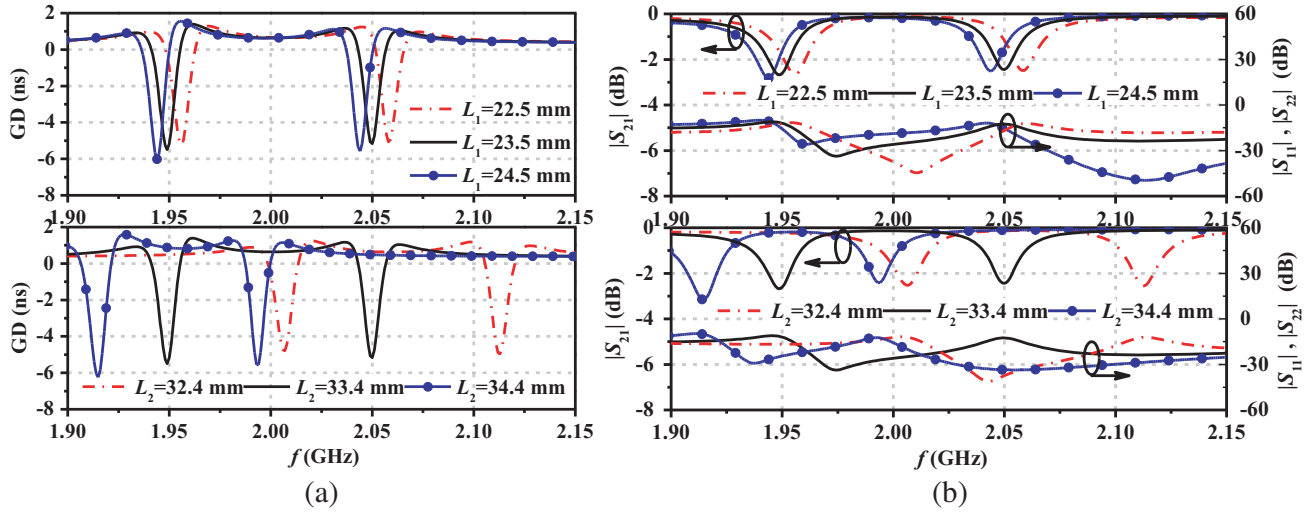

Figure 5. Effect of L_1 and L_2 on the performances of the proposed dual-band NGDC. (a) GD. (b) S-parameters.

due to the connecting lines, referring to Figs. 2 and 5.

6) Tune W_1 and W_2 according to Fig. 4 to obtain the desired frequencies f_1 and f_2.

7) Adjust W_{c1}, S_1, and S_2 referring to Figs. 2 and 3 to achieve the needed NGD times at f_1 and f_2.

3. IMPLEMENTATION AND PERFORMANCE

To validate the design concept, two dual-band NGDCs are designed and fabricated on a substrate with relative permittivity $\varepsilon_r = 2.55$ and thickness $h = 1.5$ mm. The HFSS EM software is used to obtain the optimized dimensions. The final dimensions of prototypes I and II are given in Table 1. Photographs of the fabricated prototypes are shown in Fig. 6. The circuit size of the prototypes is 70.6 mm $\times$ 46.6 mm (around $0.67\lambda_g \times 0.44\lambda_g$, where λ_g is the guided wavelength of 50-Ω transmission line at f_1). The fabricated prototypes are measured with an Agilent N5230A network analyzer.

Table 1. Dimensions of the proposed dual-band NGDC prototypes (unit: mm, referring to Fig. 1).

Prototypes	W_1	S_1	S_2	W_{c1}	W_{c2}	W_0	W_2	W_3	W_4	L_0	L_1	L_2	L_3	L_4
I	2.88	1.65	1.8	1.8	3.9	4.1	4.3	0.5	1.0	10.0	23.3	66.8	7.8	2.0
II	2.50	2.00												

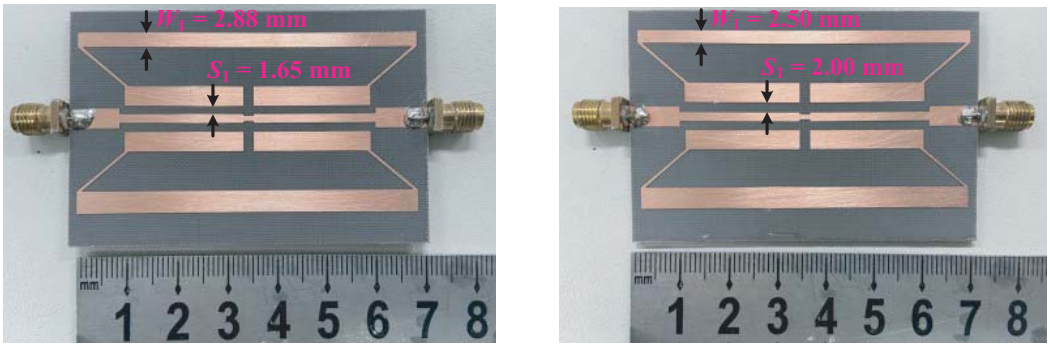

(a) (b)

Figure 6. The photograph of the fabricated dual-band NGDCs. (a) Prototype I. (b) Prototype II.

Figure 7 shows the simulated and measured results of prototype I. For the lower NGD band, the measured GD and $|S_{21}|$ at $f_1 = 1.949$ GHz are -4.9 ns and -2.6 dB, respectively. The fractional bandwidth (FBW) for GD less than 0 ns is 0.46% (1.945–1.954 GHz). For the upper NGD band, the measured GD and $|S_{21}|$ at $f_2 = 2.054$ GHz are -4.8 ns and -2.7 dB, respectively. The NGD fractional bandwidth is 0.54% (2.047–2.058 GHz). The measured return loss (RL) of both NGD bands is better than 11.2 dB (i.e., $|S_{11}| < -11.2$ dB).

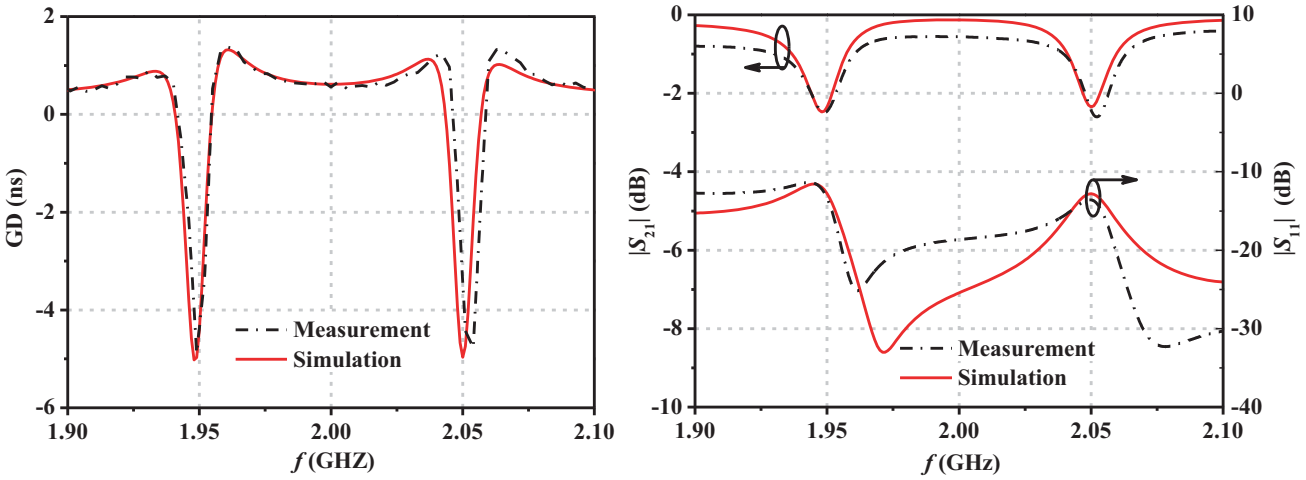

(a) (b)

Figure 7. Simulated and measured results of the proposed dual-band NGDC prototype I. (a) GD. (b) S-parameters.

For demonstrating the flexible design of the proposed dual-band NGDC (i.e., the NGD times and center frequencies of the NGD bands can be tuned independently), prototype II is designed with only change of W_1 and S_1 (as shown in Table 1) for $f_1 = 1.949$ GHz and $f_2 = 2.086$ GHz. The simulated

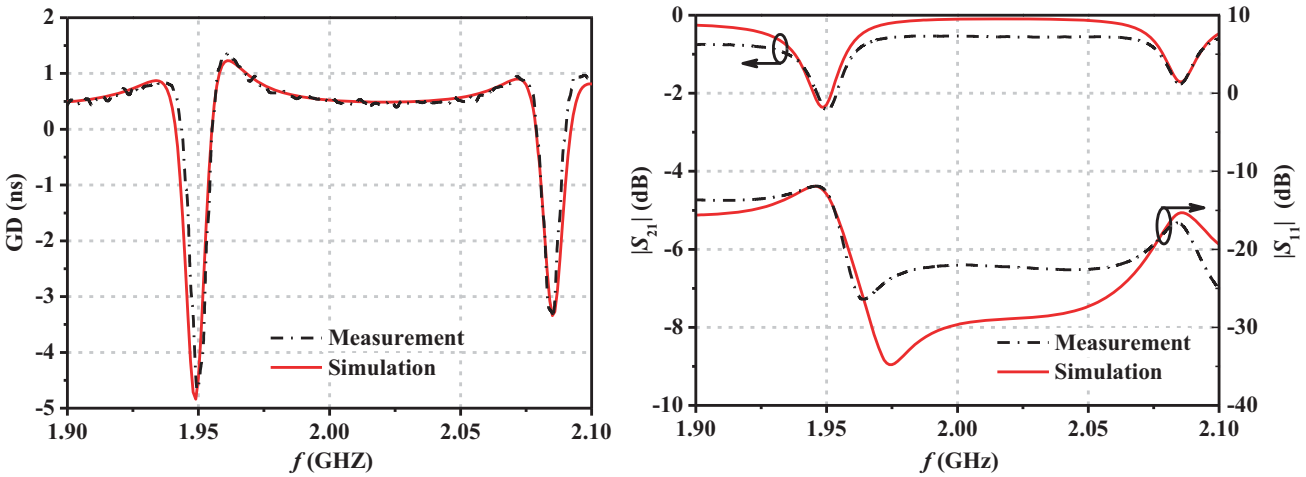

Figure 8. Simulated and measured results of the proposed dual-band NGDC prototype II. (a) GD. (b) S-parameters.

and measured GD and S-parameters of prototype II are shown in Fig. 8. The measured GD and $|S_{21}|$ at $f_1 = 1.949$ GHz are -4.7 ns and -2.4 dB, respectively. The FBW of the lower NGD band is 0.46% (1.945–1.954 GHz). The measured RL is better than 11.9 dB in the lower NGD band. For the upper NGD band, the measured GD and $|S_{21}|$ at $f_2 = 2.086$ GHz are -3.3 ns and -1.8 dB, respectively. The NGD fractional bandwidth is 0.53% (2.081–2.092 GHz). The measured RL is better than 16.6 dB in the upper NGD band.

Table 2. Performance comparison.

Ref.	f_i (GHz)	NGD (ns)	IL (dB)	RL (dB)	NGD FBW (%)	FOM	Size ($\lambda_g \times \lambda_g$)	Flexible Design
[14]	2.140	−3.0	34.2	17.0	8.41	0.0105	1.80 × 0.09	No
	3.500	−3.1	34.9	17.0	5.14	0.0100		
[16]	0.667	−1.2	18.2	24.8	34.5	0.0338	0.27 × 0.13	No
	1.377	−1.2	18.2	24.7	16.5	0.0332		
[17]	0.496	−2.9	8.30	23.3	7.66	0.0426	0.50 × 0.19	No
	1.499	−3.1	10.2	25.4	3.67	0.0519		
[18]	3.500	−4.5	47.4	-	3.43	0.0023	0.64 × 0.36	Yes
	5.150	−4.2	38.8	-	1.94	0.0048		
[19]	3.500	−5.0	13.0	-	5.71	0.2237	0.64 × 0.60	No
	5.200	−5.0	19.5	-	5.77	0.1589		
[20]	2.436	−4.1	2.13	12.6	0.49	0.0381	1.47 × 1.26	No
	3.022	−3.8	2.86	12.4	0.43	0.0358		
Prototype I	1.949	−4.9	2.60	11.2	0.46	0.0327	0.67 × 0.44	Yes
	2.054	−4.8	2.70	12.8	0.54	0.0387		
Prototype II	1.949	−4.7	2.40	12.2	0.46	0.0320	0.67 × 0.44	
	2.086	−3.3	1.80	16.9	0.53	0.0295		

Table 2 shows the comparison of the proposed NGDC with previous dual-band designs. Compared with [14, 16–20], the proposed circuit has a lower IL with a moderate RL, circuit size, and figure of merit (FOM), where the FOM is defined as

$$\text{FOM} = |\text{NGD}(f_i)| \times \text{BW}_{\text{NGD}} \times |S_{21}(f_i)| \tag{1}$$

Furthermore, the proposed dual-band NGDC has a flexible design of operation frequencies (f_1 and f_2) and NGD times.

4. CONCLUSIONS

In this paper, a novel low-loss dual-band NGDC has been presented. The proposed circuit is composed of two step-impedance open-loop resonators and a transmission line connecting input/output ports. Two dual-band NGDCs have been designed, fabricated, and measured. The measurement results are consistent with the simulation ones, which verifies the proposed NGDC with a flexible design of the operation frequencies and NGD times. In addition, the proposed NGDC has a lower IL than previous designs [14, 16–20]. So it can be applied in various dual-band microwave circuits and systems.

ACKNOWLEDGMENT

This work was supported by the National Natural Science Foundation of China (Nos. 61871417 and 51809030), the Natural Science Foundation of Liaoning Province (Nos. 2019-MS-024 and 2020-MS-127), the LiaoNing Revitalization Talents Program (Nos. XLYC2007024 and XLYC2007067), and the Fundamental Research Funds for the Central Universities (Nos. 3132021234 and 3132021231).

REFERENCES

1. Ravelo, B., S. Lalléchère, A. Thakur, A. Saini, and P. Thskuret, "Theory and circuit modeling of baseband and modulated signal delay compensations with low- and band-pass NGD effects," *AEU Int. J. Electron. Commun.*, Vol. 70, No. 9, 1122–1127, Sept. 2016.
2. Eudes, T. and B. Ravelo, "Cancellation of delays in the high-rate interconnects with UWB NGD active cells," *Appl. Phys. Res.*, Vol. 3, No. 2, 81–88, Nov. 2011.
3. Ahn, K., R. Ishikawa, and K. Honjo, "Group delay equalized UWB InGaP/GaAs HBT MMIC amplifier using negative group delay circuits," *IEEE Trans. Microwave Theory Tech.*, Vol. 57, No. 9, 2139–2147, Sept. 2009.
4. Ravelo, B., "High-pass negative group delay RC-network impedance," *IEEE Trans. Circuits Syst. II — Express Briefs*, Vol. 64, No. 9, 1052–1056, Sept. 2017.
5. Shao, T., Z. Wang, S. Fang, H. Liu, and S. Fu, "A compact transmission-line self-matched negative group delay microwave circuit," *IEEE Access*, Vol. 5, 22836–22843, Nov. 2017.
6. Xiao, J. K., Q. F. Wang, and J. G. Ma, "Matched NGD circuit with resistor-connected coupled lines." *Electron. Lett.* Vol. 55, No. 16, 903–905, Aug. 2019.
7. Chaudhary, G. and Y. Jeong, "A design of compact wideband negative group delay network using cross coupling," *Microw. Opt. Technol. Lett.*, Vol. 56, No. 11, 2612–2616, Nov. 2014.
8. Wu, Y., H. Wang, Z. Zhuang, Y. Liu, Q. Xue, and A. A. Kishk, "A novel arbitrary terminated unequal coupler with bandwidth-enhanced positive and negative group delay characteristics," *IEEE Trans. Microwave Theory Tech.*, Vol. 66, No. 5, 2170–2184, May 2018.
9. Zhang, T., T. Yang, and P. Chi, "Novel reconfigurable negative group delay circuits with independent group delay and transmission loss/gain control," *IEEE Trans. Microwave Theory Tech.*, Vol. 68, No. 4, 1293–1303, Apr. 2020.
10. Ravelo, B., F. Wan, N. Li, Z. Xu, P. Thakur, and A. Thakur, "Diakoptics modelling applied to flying bird-shape NGD microstrip circuit," *IEEE Trans. Circuits Syst. II — Express Briefs*, Vol. 68, No. 2, 637–641, Feb. 2021.

11. Wan, F., L. Wu, B. Ravelo, and J. Ge, "Analysis of interconnect line coupled with a radial-stub terminated negative group delay circuit," *IEEE Trans. Electromagn. Compat.*, Vol. 62, No. 5, 1813–1821, Oct. 2020.
12. Wan, F., N. Li, B. Ravelo, and J. Ge, "O=O shape low-loss negative group delay microstrip circuit," *IEEE Trans. Circuits Syst. II — Express Briefs*, Vol. 67, No. 10, 1795–1799, Oct. 2020.
13. Ravelo, B., N. Li, F. Wan, and J. Feng, "Design, modeling and synthesis of negative group delay IL-shape topology," *IEEE Access*, Vol. 7, 153900–153909, Oct. 2019.
14. Choi, H., Y. Jeong, J. Lim, S. Eom, and Y. Jung, "A novel design for a dual-band negative group delay circuit," *IEEE Microwave Wireless Compon. Lett.*, Vol. 21, No. 1, 19–21, Jan. 2011.
15. Ravelo, B. and S. Blasi, "An FET-based microwave active circuit with dual-band negative group delay," *J. Microw. Optoelectron. Electromagn. Appl.*, Vol. 10, No. 2, 355–366, Dec. 2011.
16. Shao, T., S. Fang, Z. Wang, and H. Liu, "A compact dual-band negative group delay microwave circuit," *Radioengineering*, Vol. 27, No. 4, 1070–1076, Dec. 2018.
17. Meng, Y., Z. Wang, S. Fang, T. Shao, H. Liu, and Z. Chen, "Dual-band negative group delay microwave circuit with low signal attenuation and arbitrary frequency ratio," *IEEE Access*, Vol. 8, 49908–49919, Mar. 2020.
18. Chaudhary, G., Y. Jeong, and J. Lim, "Miniaturized dual-band negative group delay circuit using dual-plane defected structures," *IEEE Microwave Wireless Compon. Lett.*, Vol. 24, No. 8, 521–523, Aug. 2014.
19. Taher, H. and R. Farrell, "Dual wide-band miniaturized negative group delay circuit using open circuit stubs," *Microwave Opt. Technol. Lett.*, Vol. 60, No. 2, 428–432, Feb. 2018.
20. Zhou, X., B. Li, B. Ravelo, X. Hu, et al., "Analytical design of dual-band negative group delay circuit with multi-coupled lines," *IEEE Access*, Vol. 8, 72749–72756, Apr. 2020.